Theory of autoionization and photoionization in two-electron spherical quantum dots

Y. Sajeev and N. Moiseyev*
Schulich Faculty of Chemistry and Minerva Center for Nonlinear Physics of Complex Systems, Technion-Israel Institute of Technology, Haifa 32000, Israel

(Received 24 June 2008; revised manuscript received 23 July 2008; published 20 August 2008)

The two-electron resonance states of spherically symmetric artificial atoms (quantum dots) are investigated using the complex scaled full configuration-interaction method. The one-electron confining potential term of the quantum dot is presented by a Gaussian one-electron confining potential. Contrary to natural atoms, the single electron excited states of an artificial atom become resonance states for appropriately chosen external confining potential parameters. Moreover, the external confining potential of an artificial atom can be tuned to provide efficient photodetectors, which are extremely sensitive even to a weak external radiation with a specific wavelength. In order to illustrate efficiency of such a photodetector, we calculate the ionization rates corresponding to the interaction of an artificial atom with external laser field. The mechanism for photoionization through a short-lived autoionizing singly excited resonance state is discussed.

DOI: 10.1103/PhysRevB.78.075316 PACS number(s): 73.22.−f, 31.15.ac, 73.21.La

I. INTRODUCTION

Considerable interest is currently being invested into an experimental fabrication and investigation of nanostructures known as quantum dots (QDs).[1–3] The quantum dots, consisting of several electrons moving in an external confining potential, are often described as artificial atoms since they exhibit electronic and optical properties analogous to natural atoms.[4–7] However, unlike the natural atoms, the artificial atoms can be manufactured in a controllable way to allow the precise tuning of a variety of parameters such as the number of electrons in the external confining potential.[1,2]

One of the substantial differences between natural and artificial atoms consists in the fact that in natural atoms the singly excited electronic states are always bound while in artificial atoms, they may become resonance states for an appropriately tailored width and depth of the external confining potential. Hence, it is of considerable interest to try to extend the previously pursued theoretical investigations of bound states of artificial atoms[8–11] to the case of metastable autoionizing resonance states. Bylicki *et al.*[12] calculated the resonance states of two-electron finite rectangular well quantum dots by using a complex scaling method (see references in Refs. 13 and 14). Note by passing that the complex scaling transformation they have used in their calculations is not justified for a piecewise (non-dilation-analytic) potential, and that the exterior scaling method[15] or the smooth exterior scaling transformation[16] should be used in this case.

As already mentioned before, from a theoretical point of view an artificial atom can be constructed via replacing the electron-nucleus attractive potential of a natural atom by some other one-electron external confining potential. In most theoretical model calculations a parabolic confining potential has been used. One advantage of the parabolic confining potentials is that they fulfill the generalized Kohn theorem, which asserts that an excitation spectrum related to the optical and magneto optical absorptions has no connection with the electron-electron interaction.[17] On the other hand, the parabolic potential has also certain limitations. Since it possesses an infinite depth, it cannot take into account the autoionization and photoionization phenomena. Recently, an inverse Gaussian confining potential that possesses a finite depth has been found appropriate for numerical studies of artificial atoms.[18,19] The mentioned Gaussian potential takes the form

$$V(\vec{q}) = -\tilde{V}_0 \exp(-\tilde{\beta}\vec{q}^2), \tag{1}$$

and is characterized by a finite depth ($\tilde{V}_0$) and a potential width parameter ($\tilde{\beta}$). The width parameter $\tilde{\beta}$ can be related to the radius R at half height of the quantum dot potential,

$$R = \sqrt{\frac{\ln 2}{\tilde{\beta}}}. \tag{2}$$

By adjusting the parameters $\tilde{V}_0$ and $\tilde{\beta}$ of the Gaussian confining potential [Eq. (1)], the single electron excited bound state and even the ground electronic state, which are corresponding to specific values of $\tilde{\beta}$, are turned into autoionizing states for other values of $\tilde{\beta}$. In the present work, we focus on the single electron excited resonance states in two-electron quantum dot ($2e$-QD), and study their properties as a function of $\tilde{V}_0$ and $\tilde{\beta}$. We study also the effect of single electron excited autoionizing states on the photoionization decay rate as the artificial atom is exposed to external laser field. A photoionization occurs when an electron is excited from the ground state to the continuum. This photoionization mechanism requires relatively strong laser field intensities since the relevant bound-continuum transition dipole moments possess small values due to the delocalized nature of the continuum states. In the present work, we propose another photoionization mechanism that is very different from the one described above. Our proposed mechanism is based on the fact that, unlike in real atoms, the single electron excited states of a quantum dot can be designed to be autoionizing resonance states by adjusting the parameters $\tilde{V}_0$ and $\tilde{\beta}$ of the Gaussian confining potential. The finite lifetime of the single electron excited states in $2e$-QD results from the repulsion that "kicks" one of the electrons out of the QD's

potential well in order to stabilize the system. Such single electron excited autoionizing states are spatially localized inside the Gaussian confining potential (similarly to the bound ground state) in spite of the fact that they have finite lifetimes. Hence, the bound-resonance transition dipole moments have similar magnitude to the bound-bound transition moments, i.e., much larger than the bound-continuum counterparts. Thus, by using a laser with suitable frequency that couples the ground state with an autoionizing single electron excited state, the photoinduced ionization rate of decay can be dramatically enhanced. Our intention is to design efficiently controlled photodetectors by varying the shape of the artificial Gaussian confining potential.

The paper is organized as follows. Section II contains a brief outline of the *ab initio* electronic structure methods that are used for the calculation of energy and lifetime of single electron excited autoionizing resonance states in $2e$-QDs. We also briefly describe the Floquet theory,[20] which is used for the calculation of photoionization decay rate when the QD interacts with a linearly polarized laser field. In Sec. III we specify the construction of the basis sets and other computational details. Finally, in Sec. IV we present and discuss our results for the resonance position (energy) and width (inverse lifetime) of single electron excited autoionizing states in the field-free $2e$-QD, and the photoinduced ionization rate of decay for $2e$-QD in its ground state, which is exposed to a moderate/weak linearly polarized laser field. Concluding remarks are given in Sec. V.

II. THEORY METHODS

The time dependent Hamiltonian, within framework of the effective-mass formalism, of two electrons in a Gaussian confining potential system that interact with an external linearly polarized laser field is given by

$$\hat{H}(m_e^*,\tilde{V}_0,\tilde{\beta},\tilde{\kappa},\vec{q}_1,\vec{q}_2,\tilde{\varepsilon}_0,\omega,t) = \hat{H}_{FF}(m_e^*,\tilde{V}_0,\tilde{\beta},\tilde{\kappa},\vec{q}_1,\vec{q}_2) - \tilde{\varepsilon}_0\vec{e}_z(\vec{q}_1+\vec{q}_2)\cos(\omega t), \tag{3}$$

where the laser-matter interaction term is expressed in the length gauge using the dipole approximation, ω is the frequency of the laser light, ε_0 is the maximum field amplitude of the laser light, and $\vec{e}_z$ is a unit vector perpendicular to the light propagation axis. $\hat{H}_{FF}(m_e^*,\tilde{V}_0,\tilde{\beta},\tilde{\kappa},\vec{q}_1,\vec{q}_2)$ stands for the field-free Hamiltonian for the $2e$-QD and is defined as

$$\hat{H}_{FF}(m_e^*,\tilde{V}_0,\tilde{\beta},\kappa,\vec{q}_1,\vec{q}_2) = -\sum_{i=1}^{2}\frac{1}{2m_e^*}\nabla_i^2 - \sum_{i=1}^{2}V_0\exp(-\tilde{\beta}q_i^2) + \frac{1}{\kappa|\vec{q}_1-\vec{q}_2|}, \tag{4}$$

where m_e^* is the effective mass of an electron in the QD and κ is the effective dielectric constant of the QD. By scaling the electronic coordinates with κ/m_e^*, it can be shown that

$$\hat{H}(m_e^*,\tilde{V}_0,\tilde{\beta},\kappa,\vec{q}_1,\vec{q}_2,\tilde{\varepsilon}_0,\omega,t) = \frac{m_e^*}{\kappa^2}\hat{H}(1,V_0,\beta,1,\vec{r}_1,\vec{r}_2,\varepsilon_0,\omega,t), \tag{5}$$

where

$$\vec{r} = \vec{q}\frac{\kappa}{m_e^*}, \tag{6}$$

$$V_0 = \tilde{V}_0\frac{\kappa^2}{m_e^*}, \tag{7}$$

$$\beta = \tilde{\beta}\frac{\kappa^2}{m_e^{*2}}, \tag{8}$$

and

$$\varepsilon_0 = \tilde{\varepsilon}_0\frac{\kappa^3}{m_e^2}. \tag{9}$$

Throughout the present paper, we use the transformed Hamiltonian $\hat{H}(1,V_0,\beta,1,\vec{r}_1,\vec{r}_2,\varepsilon_0,\omega,t)$, where the scaled Hartree units are defined as follows: energy in the units of m_e^*/κ^2, length in the units of κ/m_e^*, V_0 in the units of κ^2/m_e^*, β in the units of κ^2/m_e^{*2}, and ε_0 in the units of κ^3/m_e^2. Let us now discuss the main significant theoretical steps of our numerical calculations.

A. Calculation of autoionizing resonance energies and widths (inverse lifetimes) in two-electron quantum dot

As stated in the Sec. I, we use complex scaling method to calculate the energies and widths (inverse lifetimes) of single electron excited states in $2e$-QD. The calculation of lifetime and energies becomes simpler by the use of complex scaling method, which enables us to calculate the resonance by computational methods that originally have been developed for the calculation of bound states. The fundamental works by Balslev and Combes,[21] and by Simon[22] have provided the underlying mathematical foundations. The associated complex scaled field-free Schrödinger equation can be written as

$$H_{FF}^{(\eta)}|\varphi_j^{(\eta)}\rangle = E_j^{\eta}|\varphi_j^{(\eta)}\rangle, \tag{10}$$

where the dilation transformation $r\rightarrow r\eta$, using a complex scaling parameter $\eta=e^{i\theta}$, is applied for the electronic coordinates. Within the complex scaling approach, the resonance position (energies) E_j^{res} and the widths Γ_j are associated with the complex eigenvalues, $E_j^{\eta}=E_j^{\mathrm{res}}-i\Gamma_j/2$, of the complex scaled Hamiltonian. The resonance wave functions become square integrable upon the complex scaling transformation. Thus, the complex scaling method has the fundamental advantage of associating a resonance state with a wave function that is embedded in the generalized Hilbert space rather than with a wave packet (i.e., a collection of continuum eigenstates of the unscaled Hermitian Hamiltonian).[13,14] In our numerical calculation η is taken as $\eta=\alpha e^{i\theta}$, where α and θ are real variables. Our choice of the basis functions will be described in Sec. III. The resonance complex eigenvalues are

associated with stationary solutions in the complex variational space such that

$$\left.\frac{dE_j^{\eta}}{d\eta}\right|_{\eta=\eta_{\rm opt}} = 0, \tag{11}$$

and

$$\eta_{\rm opt} = |\alpha_{\rm opt}| e^{i\theta_{\rm opt}}. \tag{12}$$

Since E_j^{η} is a complex function, there is a need for two nonlinear variational parameters, α and θ, in order to get stationary solution in the complex variational space. The stationary solutions are associated with a cusp in the α or θ trajectory calculations.[23] As the basis set becomes more complete, the dependence of E_j^{η} on η becomes weaker.

B. Photoionization of two-electron quantum dot that interacts with a laser

Let us assume that an artificial atom is exposed to a monochromatic laser light with a given frequency ω. Below we briefly discuss the non-Hermitian Floquet formalism, as formulated by Chu and co-workers.[24,25] For the use of the complex scaled Floquet theory in calculations of the correlated electronic photoinduced dynamics in strong laser fields, see Ref. 26.

The complex scaled time dependent Schrödinger equation can be written as follows:

$$\hat{H}^{(\eta)}\Psi_{\alpha}^{(\eta)}(t) = i\hbar\frac{\partial}{\partial t}\Psi_{\alpha}^{(\eta)}(t), \tag{13}$$

where $\hat{H}^{(\eta)}$ is the complex scaled Hamiltonian, as defined in Eq. (3). According to the Floquet theorem, there exist particular solutions $\Psi_{\alpha}^{(\eta)}(t)$ of Eq. (13) obeying an ansatz,

$$\Psi_{\alpha}^{(\eta)}(\vec{q}_1,\vec{q}_2,t) = e^{-i\varepsilon_{\alpha}^{\rm QE}t/\hbar}\Phi_{\alpha}^{(\eta)}(\vec{q}_1,\vec{q}_2,t). \tag{14}$$

Here, $\Phi_{\alpha}^{(\eta)}(\vec{q}_1,\vec{q}_2,t)$ is time periodic function with the period $T=2\pi/\omega$ and $\varepsilon_{\alpha}^{\rm QE}$ is the complex quasienergy (defined as the module of $\hbar\omega$) where the photoionization decay rate is given by $\Gamma_{\alpha}^{\rm QE}=-2\ {\rm Im}\ \varepsilon_{\alpha}^{\rm QE}$. The complex scaled Floquet eigenenergy equation can be written as

$$\hat{H}_f^{(\eta)}\Phi_{\alpha}^{(\eta)}(\vec{q}_1,\vec{q}_2,t) = \varepsilon_{\alpha}^{\rm QE}\Phi_{\alpha}^{(\eta)}(\vec{q}_1,\vec{q}_2,t), \tag{15}$$

where $\hat{H}_f^{(\eta)}$ is the complex scaled Floquet Hamiltonian,

$$\hat{H}_f^{(\eta)} = \hat{H}_{FF}^{(\eta)} - \eta\tilde{\varepsilon}_0\vec{e}_z(\vec{q}_1+\vec{q}_2)\cos(\omega t) - i\hbar\frac{\partial}{\partial t}, \tag{16}$$

and the time variable t is considered as an additional coordinate. Equation (15) can be solved by using the conventional basis set expansion techniques. The time variable t is covered by an appropriate Fourier basis set,

$$\Phi_{\alpha}^{(\eta)}(\vec{q}_1,\vec{q}_2,t) = \sum_{n=-\infty}^{\infty}\chi_{\alpha,n}^{(\eta)}(\vec{q}_1,\vec{q}_2)e^{in\omega t}. \tag{17}$$

The wave-function components $\chi_{\alpha,n}^{(\eta)}(\vec{q}_1,\vec{q}_2)$ can be further expanded using the eigenstates of $\hat{H}_{FF}^{(\eta)}$,

$$\chi_{\alpha,n}^{(\eta)}(\vec{q}_1,\vec{q}_2) = \sum_j C_{(j,n),\alpha}|\varphi_j^{(\eta)}(\vec{q}_1,\vec{q}_2)\rangle. \tag{18}$$

For the sake of clarity, we recall here that the eigenfunctions $|\varphi_j^{(\eta)}(\vec{q}_1,\vec{q}_2)\rangle$ of a non-Hermitian Hamiltonian $\hat{H}_{FF}^{(\eta)}$ satisfy the orthonormality relations only when the inner product definition is altered into c product,[27] i.e., $\langle\varphi_i^{(\eta)*}(\vec{q}_1,\vec{q}_2)|\varphi_j^{(\eta)}(\vec{q}_1,\vec{q}_2)\rangle=\delta_{i,j}$. After substituting Eqs. (18) and (17) into Eq. (15), and acting with $1/T\int_0^T dt\langle\varphi_i^{(\eta)*}(\vec{q}_1,\vec{q}_2)e^{-im\omega t}|$, one obtains the matrix eigenvalue problem,

$$\mathbf{H}_f\mathbf{C} = \boldsymbol{\varepsilon}^{\rm QE}\mathbf{C}, \tag{19}$$

where the matrix elements of the Floquet matrix are given by

$$[H_f(\eta)]_{(i,m)(j,n)} = (E_j^{\eta} - n\hbar\omega)\delta_{mn}\delta_{ij} - \frac{\varepsilon_0 e^{i\theta}}{2}\langle\varphi_i^{(\eta)*}(\vec{q}_1,\vec{q}_2)|\vec{e}_z(\vec{q}_1+\vec{q}_2)| \times\varphi_j^{(\eta)}(\vec{q}_1,\vec{q}_2)\rangle\delta_{m,n\pm1}. \tag{20}$$

Equation (19) is solvable by using conventional numerical techniques for diagonalization of complex symmetric matrices.

III. COMPUTATIONAL DETAILS

A. Choice of the basis sets

Our calculations of the field-free resonances are restricted to S and P states. We use a polarized valence correlation consistent quadruple zeta (cc-pVQZ) (Ref. 28) Gaussian basis set for the two-electron problem as the parent basis set. For an adequate description of the ground-state and resonance-state wave functions, successive augmentation of the above mentioned parent cc-pVQZ basis set has been done with separate sets of diffused basis sets, as being specified below.

For the S states of the Gaussian confining potential, we augmented the parent cc-pVQZ basis set with a set of s, p, and d functions. The resulting augmented cc-pVQZ (Ref. 28) basis set is further augmented with s-, p-, and d-type even-tempered Gaussian basis functions. The exponents of these even-tempered basis functions are calculated using the formula

$$\alpha_i^{s,p,d} = (\varepsilon^{s,p,d})^{1/N^{s,p,d}}\alpha_{i-1}^{s,p,d}, \tag{21}$$

where N is the total number of even-tempered Gaussians used for augmentation. In order to make the whole basis set as linearly independent, we have taken α_0 to be the same as the orbital exponent of the most diffused basis function. More specifically, the exponents of the additional even-tempered Gaussians for the S states are calculated by taking

$$\alpha_0^s = 0.04819, \quad \varepsilon^s = 1\times10^{-3}, \quad N^s = 15,$$

$$\alpha_0^p = 0.1626, \quad \varepsilon^p = 5\times10^{-3}, \quad N^p = 5,$$

$$\alpha_0^d = 0.3510, \quad \varepsilon^d = 1 \times 10^{-2}, \quad N^d = 3. \tag{22}$$

For the P state of the artificial atom, we have augmented the parent cc-pVQZ basis set with a set of even-tempered Gaussians using

$$\alpha_0^s = 0.1833, \quad \varepsilon^s = 1 \times 10^{-3}, \quad N^s = 10,$$

$$\alpha_0^p = 0.5600, \quad \varepsilon^p = 1 \times 10^{-3}, \quad N^p = 10,$$

$$\alpha_0^d = 1.2230, \quad \varepsilon^d = 1 \times 10^{-3}, \quad N^d = 3. \tag{23}$$

These diffused even-tempered basis functions are added to standard correlation consistent basis set, which has been discussed above. This particular basis set proved to provide well converged energy eigenvalues for the entire set of Gaussian confining potentials under our study.

B. Representation of the complex scaled field-free electronic Hamiltonian

The complex scaled Schrödinger equation for a $2e$-QD confining potential is simple enough to be solved by the use of the full configuration-interaction (FCI) method. By employing the successive FCI procedures for continuous change of the width parameter of the Gaussian confining potential ($\tilde{\beta}$), the transition of bound states into resonance states can be studied. The reference orbitals for the FCI calculations were obtained from a standard restricted Hartree-Fock calculation for the ground state of the Hermitian (unscaled) Hamiltonian of the $2e$-QD. Using these Hartree-Fock unscaled orbitals, we constructed the ground state and all the possible singly excited and doubly excited two-electron Slater determinants. These determinants were used as a basis set in the FCI calculations of the eigenvalues and eigenfunctions of the complex scaled Hamiltonian. We have used 2176 Slater determinants with Ag symmetry and 1258 Slater determinants with B1u symmetry for the FCI calculation. The symmetric notations Ag and B1u were taken from the $d2h$ subgroup of the spherically symmetric system. The intermediate Hartree-Fock calculation helps us to construct an orthogonal basis set for the FCI calculation rather than using nonorthogonal primitive Gaussian basis functions. The matrix representation of the complex scaled Hamiltonian of the $2e$-QD associated with the kinetic-energy operator, the electron-electron Coulombic repulsion, and the dipole operator were calculated using the GAMESS-U.S. QUANTUM CHEMICAL PACKAGE[29] with the basis set described above. The matrix elements associated with the complex scaled Gaussian confining potential were calculated analytically.

C. Solution of the Floquet problem

The ^1S (ground state) and the lowest ^1P field-free electronic states were used as basis functions in the calculation of non-Hermitian Floquet states. The diagonalization of the complex scaled Floquet matrix has been carried out by using $(N+1)$ number of Fourier basis functions, $\exp(-in\omega)$, where $n=0, \pm 1, \ldots \pm N/2$. In our calculations we checked for the convergence by increasing the value of N. The reported energy values are converged for $N=4$ (five Fourier basis functions).

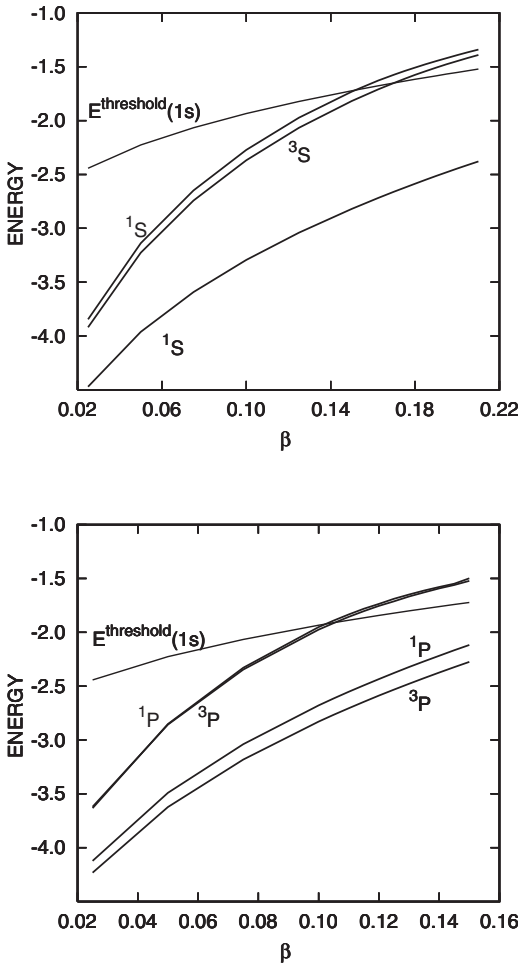

FIG. 1. The positions of the S- and P-type resonance energies plotted as a function of the width parameter of the Gaussian confining potential. The bound-autoionizing resonance transformation occurs at the values of β where the bound energy levels cross the $E^{\text{threshold.}}$ curve (i.e., the energy of a single electron quantum dot). Energies and widths of the Gaussian confining potential parameter, β, are given in scaled Hartree units. For conversion factors to Hartree units, see Eqs. (5)–(9).

IV. RESULTS AND DISCUSSION

In Figs. 1 and 2 we show our results for the energy positions and widths (inverse lifetime) of the autoionizing states, plotted as functions of the width parameter of the Gaussian confining potential (β) for $V_0=3$ (in scaled Hartree units), where β is varied from 0.02 to 0.22 (in scaled Hartree units). For example, in the case of GaAs quantum dots, the effective mass is equal to 0.067 Hartree units and the dielectric constant is equal to 12.4 Hartree units. Therefore, the depth of the QD potential that has been used in our calculation is 0.001 307 Hartree units and β has been varied from 57.656 ($\beta=0.02$ scaled Hartree units) to 17.38 nm ($\beta=0.22$ scaled Hartree units).

For illustrational reasons, we plot in Fig. 1 also the first ionization threshold as functions of β. As it is shown in Fig.

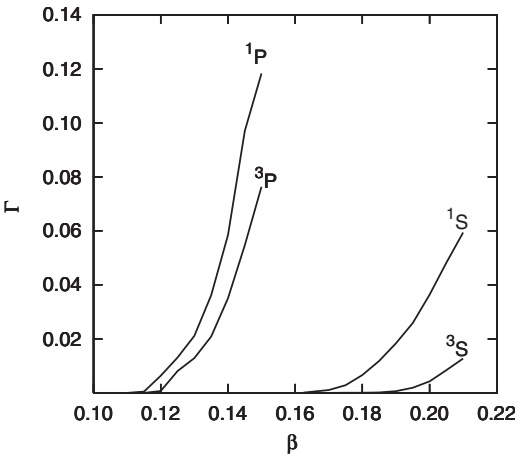

FIG. 2. The widths (inverse lifetimes) of the S- and P-type autoionizing resonance states as a function of the width parameter of the Gaussian confining potential β. Note that only for sufficiently large values of β that exceed critical values associated with the curve crossings shown in Fig. 1 are the bound states turned into autoionizing states. Γ and β are given in scaled Hartree units. For conversion factors to Hartree units, see Eqs. (5)–(9).

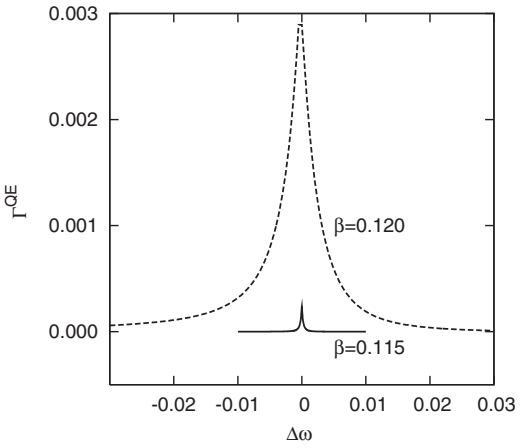

FIG. 3. Photoionization decay rate of the ground state ^1S of $2e$-QD that is exposed to a linearly polarized laser light with the laser frequency ω. The resonance condition is when $\Delta\omega=0$ (i.e., the field-free excitation energy is equal to a single-photon energy $\hbar\omega$). The photoionization decay rate obtained for $\beta=0.115$ (in scaled Hartree units) when the ^1P excited state is a bound state. The results obtained for $\beta=0.120$ (in scaled Hartree units) are when the ^1P excited state is an autoionizing resonance state. The photoionization decay rate $\Delta\omega$ and β are given in scaled Hartree units.

1 by squeezing the Gaussian potential, the singly excited bound electronic states cross the first ionization threshold and become autoionizing resonance states. The corresponding resonance widths increase as the width parameter of the Gaussian potential, β, is further reduced. The singlet states decay somewhat faster than the corresponding triplet states due to the electron-electron repulsion energy, which is higher than the electron-electron repulsion energy for the triplet state in the $2e$-QD.[30] In Fig. 1 we show how the low laying singly excited states are transformed into resonance states by varying β (i.e., by varying the radius of the QD). From the results presented in Fig. 2, one can see that, when the excited state gets above the first threshold energy (see Fig. 1), the excited state becomes an autoionizing state with finite lifetime, which is equal to $\hbar/\Gamma$.

Let us discuss now the use of our numerical Floquet calculations in the calculation of photoinduced ionization in $2e$-QD. The initial state is the ground ^1S state of the $2e$-QD. The linearly polarized laser light excites the $2e$-QD into ^1P autoionizing resonance state. Five Floquet channels were used to get the converged results, which are presented in Fig. 3. In Fig. 3 the frequency of the laser is varied around the resonance frequency corresponding to the $^1S \rightarrow {}^1P$ excitation energy while the field intensity is held fixed at the value that gives the maximum ionization rate for the resonance condition; i.e.,

$$\Delta\omega = \left(\frac{E_{^1P}^{FF} - E_{^1S}^{FF}}{\hbar} - \omega \right) = 0. \tag{24}$$

The dashed curve gives the rate of ionization corresponding to the Gaussian confining potential parameters $V_0=3$ (in scaled Hartree units) and $\beta=0.120$ (scaled Hartree units), and the full curve gives the ionization rate corresponding to the Gaussian confining potential parameters $V_0=3$ (in scaled Hartree units) and $\beta=0.115$ (in scaled Hartree units). For the case of GaAs quantum dots, the strength parameter corresponding to $V_0=3$ scaled Hartree units is $V_0=0.00131$ Hartree, and the quantum dot radii corresponding to $\beta=0.120$ (in scaled Hartree units) and $\beta=0.115$ (in scaled Hartree units) are 444.8 and 454.4 nm, respectively. The electronic state corresponding to the singly excited $1s2p$ reference state has been changed from a bound state to a resonance state as one increases the value of β. The bound-resonance transition of the electronic state $1s2p$ occurs for $120 > \beta > 0.115$ (in scaled Hartree units). Therefore, Γ^{QE} that were obtained for β value close to 0.115 (in scaled Hartree units) results from a multiphoton absorbing process since ^1P state is still a bound excited state. Whereas, the photoionization rate of decay Γ^{QE} that were obtained for $\beta=0.120$ (in scaled Hartree units) is mainly a single-photon phenomenon since the ^1P is an autoionizing resonance state. The maximum field amplitudes that are required in order to get the maximum ionization rate for $\beta=0.115$ (in scaled Hartree units) and $\beta=0.120$ (in scaled Hartree units) at resonance condition, $\Delta\omega=0$, are $\varepsilon_0=0.0021$ (in scaled Hartree units) and $\varepsilon_0=0.0314$ (in scaled Hartree units) units, respectively. For the case of GaAs quantum dots, the corresponding intensities are 3.64×10^6 and 8.19×10^8 W/cm^2, respectively. It is clear that the use of resonance autoionization $1s2p$ as an intermediate state in the photoinduced process is more efficient than the use of the bound-continuum mechanism. However, not only the ionization rate that uses the autoionization state as an intermediate state by more than one order of magnitude more efficient than the use of bound-continuum mechanism but it also is more sensitive to an external week radiation. Note that the maximal value of the photoionization decay rate as a function of β for $\Delta\omega=0$ (i.e., resonance peak in Fig. 3) is about equal to half of the values of the decay rate of field-free ^1P autoionizing resonance, state which are shown

in Fig. 2. This resonance photoionization mechanism is particularly useful in designing the photodetectors as we will explain below.

V. CONCLUDING REMARKS

We have calculated the transition of bound singly excited states to autoionizing resonance states by decreasing the radius of the Gaussian confining potential while using the fully correlated *ab initio* electronic structure methods (FCI). As the laser is turned on, the field-free bound ground state is tuned to a metastable resonance photoionizing state due to the dipole coupling either to the field-free autoionizing singly excited ^1P state or to the nonresonance continuum. This is a key point in our proposition for the construction of photodetectors that are sensitive to an external radiation. The field-free autoionizing ^1P resonance state, which is used as an intermediate state in the photoionization process, is well localized inside the Gaussian confining potential, similarly to the bound states of real atoms. Therefore, the electric-dipole bound-autoionizing resonance matrix elements are much larger than the bound-continuum dipole matrix elements. The electronic correlation plays a very important role in our photoionization mechanism. Due to the fact that both the bound and the resonance states are localized in the same spatial region, the dipole transition matrix element is dramatically enhanced when the laser frequency is chosen to couple the bound ground state with an autoionizing resonance state rather than with a nonresonance continuum state.

ACKNOWLEDGMENTS

The authors acknowledge Oded Shemer for his help in the preliminary steps of the numerical calculations. The authors would like to thank Dr. Milan Sindelka for various fruitful and most helpful discussions, and for his most helpful comments and suggestions. The work is supported in part by the Israel Science Foundation under Grant No. 96/07.

*nimrod@techunix.technion.ac.il

[1] S. M. Reimann and M. Manninen, Rev. Mod. Phys. **74**, 1283 (2002).
[2] A. J. Zrenner, Chem. Phys. **112**, 7790 (2000).
[3] G. Schedelbeck, W. Wegscheider, M. Bichler, and G. Abstreiter, Science **278**, 1792 (1997).
[4] R. C. Ashoori, Nature (London) **379**, 413 (1996).
[5] J. Kyriakidis, J. Phys.: Condens. Matter **17**, 2715 (2005).
[6] K. Keren, A. Stern, and U. Sivan, Eur. Phys. J. B **18**, 311 (2000).
[7] A. Fuhrer, S. Lüscher, T. Heinzel, K. Ensslin, W. Wegscheider, and M. Bichler, Phys. Rev. B **63**, 125309 (2001).
[8] I. Heidari, S. Pal, B. S. Pujari, and D. G. Kanhare, J. Chem. Phys. **127**, 114708 (2007).
[9] M. Rontani, C. Cavazzoni, D. Bellucci, and G. Goldoni, J. Chem. Phys. **124**, 124102 (2006).
[10] T. M. Henderson, K. Runge, and R. J. Bartlett, Phys. Rev. B **67**, 045320 (2003).
[11] E. Räsänen, H. Saarikoski, V. N. Stavrou, A. Harju, M. J. Puska, and R. M. Nieminen, Phys. Rev. B **67**, 235307 (2003).
[12] M. Bylicki, W. Jaskólski, A. Stachów, and J. Diaz, Phys. Rev. B **72**, 075434 (2005).
[13] W. P. Reinhardt, Annu. Rev. Phys. Chem. **33**, 223 (1982).
[14] N. Moiseyev, Phys. Rep. **302**, 212 (1998).
[15] B. Simon, Phys. Lett. **71A**, 211 (1979).
[16] N. Rom, E. Engdahl, and N. Moiseyev, J. Chem. Phys. **93**, 3413 (1990).
[17] L. Brey, N. F. Johnson, and B. I. Halperin, Phys. Rev. B **40**, 10647 (1989).
[18] J. Adamowski, M. Sobkowicz, B. Szafran, and S. Bednarek, Phys. Rev. B **62**, 4234 (2000).
[19] W. Xie, Solid State Commun. **127**, 401 (2003).
[20] G. Floquet, Ann. Sci. Ec. Normale Super. **12**, 47 (1883).
[21] E. Balslev and J. M. Combes, Commun. Math. Phys. **22**, 280 (1971).
[22] B. Simon, Commun. Math. Phys. **27**, 1 (1972); Ann. Math. **97**, 247 (1973).
[23] N. Moiseyev, S. Friedland, and P. R. Certain, J. Chem. Phys. **74**, 4739 (1981).
[24] S. I. Chu and W. P. Reinhardt, Phys. Rev. Lett. **39**, 1195 (1977).
[25] S. I. Chu and D. A. Telnov, Phys. Rep. **390**, 1 (2004).
[26] N. Moiseyev and F. Weinhold, Phys. Rev. Lett. **78**, 2100 (1997).
[27] N. Moiseyev, P. R. Certain, and F. Weinhold, Mol. Phys. **36**, 1613 (1978).
[28] D. E. Woon and T. H. Dunning, Jr., J. Chem. Phys. **100**, 2975 (1994).
[29] M. W. Schmidt, K. K. Baldridge, J. A. Boatz, S. T. Elbert, M. S. Gordon, J. H. Jensen, S. Koseki, N. Matsunaga, K. A. Nguyen, S. J. Su, T. L. Windus, M. Dupuis, and J. A. Montgomery, J. Comput. Chem. **14**, 1347 (1993).
[30] Y. Sajeev, M. Sindelka, and N. Moiseyev, J. Chem. Phys. **128**, 061101 (2008).